14th International Conference on Structural Safety and Reliability - ICOSSAR'25
June 1-6 2025
University of Southern California
Los Angeles, CA, USA

STATISTICAL LINEARIZATION-BASED OPTIMAL TUNING OF TUNED MASS NONLINEAR DAMPER INERTER FOR SEISMIC RESPONSE MITIGATION OF BUILDINGS WITH HYSTERETIC INTER-STOREY ISOLATION

K. Rajana[1] **and A. Giaralis**[1]

[1] Khalifa University of Science and Technology
Shakhbout Bin Sultan St, Hadbat Al Za`Faranah, Zone 1, Abu Dhabi, UAE
E-mail: *komal.rajana@ku.ac.ae*

Abstract

Inter-storey isolation is a passive seismic protection strategy that uses flexible bearings to create an intermediate isolated story (IS) in multi-story buildings. The system makes a versatile seismic protection strategy, particularly attractive in redevelopment and/or seismic retrofitting of dual-purpose buildings. However, several challenges arise in IS-equipped buildings, including excessive drifts of the IS. Previous studies explored the coupling of IS with linear supplemental devices like fluid viscous dampers (FVDs) and inerter-based vibration absorbers. This paper extends these efforts by optimally designing a hybrid IS system with nonlinear isolators a tuned mass nonlinear damper inerter (IS-TMDI). In the IS-TMDI system, a nonlinear FVD following a power damping force-velocity law is the primary seismic energy dissipation device. Further, the nonlinear behaviour of the isolators is captured using the Bouc-Wen model. Hence, the paper puts forth a statistical linearization (SL) approach for the optimal IS-TMDI tuning and assessment to efficiently accommodate the nonlinear terms. In this approach, the seismic excitation is modelled as a stationary filtered Kanai-Tajimi stochastic process, assuming soft soil conditions. The numerical work considers a benchmark 20-story shear frame building, with the IS-TMDI positioned at four different intermediate floors. An additional configuration with a TMDI placed at an isolated rooftop (IR-TMDI), previously introduced by the authors for seismic retrofitting of existing buildings, is further included in the comparative study. Stationary displacement response variance data obtained from SL reveal that the low-floor IS-TMDI placements are more efficient in suppressing seismic building storey drift demands, while contrary to IR-TMDI, the IS-TMDI performance is insensitive/robust to the adopted optimal tuning criterion. Further, the practically important IS displacement demands are effectively regulated by the inertance ratio of the TMDI. Thus, the reported data demonstrate good potential of the IS-TMDI for seismic protection of buildings, paving the way for further fruitful research for a variety of buildings under recorded ground motions.

Keywords: Inter-storey isolation; tuned mass damper inerter; nonlinear fluid viscous damper; statistical linearization; optimal tuning

1 INTRODUCTION

The concept of base isolation is arguably the most widely considered in practice passive vibration control strategy for the seismic protection of buildings [1], using laterally flexible bearings placed at the basement of buildings to decouple the building motion from the ground motion during earthquakes. In recent years, the use of such bearings to create an intermediate isolated story (IS) for the seismic response mitigation of multi-story buildings has found some practical application [2], being particularly attractive in redevelopment and/or seismic retrofitting of dual-purpose high-rise buildings. One possible interpretation of the latter passive vibration control configuration is to recognize that the intermediate IS may transform the superstructure (part of the building above the IS) into a large-mass tuned mass damper (TMD), leveraging its inertia to mitigate the seismic response of the substructure (part of the building below the IS) [3]. In this regard, a limiting IS configuration is the isolated rooftop (IR) configuration, in which the top floor slab (roof) rests on isolation bearings to form a TMD while fluid viscous dampers (FVDs) are additionally incorporated to increase seismic energy dissipation, thus reducing seismic building demands [4,5].

Nevertheless, the IS concept faces a main challenge of excessive deflection/drift of the isolation layer, which compromises structural safety. To this end, Liu et al. [6] examined the use of FVDs to mitigate the IS drift demands, but found that this consideration may amplify story drifts of the superstructure, which is a recurrent issue for FVD-equipped base-isolated buildings as well [7]. Therefore, more recently, Liang et al. [8] considered the use of a linear tuned mass damper inerter (TMDI) to control IS drifts and, more generally, to improve the seismic performance of IS-protected buildings. In detail, the TMDI is a passive dynamic vibration absorber introduced by Marian and Giaralis [9] for structural seismic response mitigation, coupling the conventional TMD with an inerter device that generates a relative-acceleration force proportional to its inertance property [10]. The latter device contributes large inertia (of the order of thousands of tons) without adding any significant weight, since inertance scales up practically independently from the device's physical mass [11,12]. In this respect, linear lightweight TMDI with large inertance was shown to significantly outperform the TMD for seismic response mitigation of multi-storey buildings in several studies (e.g. [13,14]), as long as the inerter extends to at least two floors below the floor where the damper is installed. However, TMDI configurations spanning multiple floors generate excessively large inerter control forces and pose practical implementation challenges. To this end, Rajana *et al*. [15] demonstrated that employing nonlinear FVDs in the TMDI reduces seismic force demands at the inerter device. Further, Rajana and Giaralis [16] coupled an IR featuring nonlinear isolators with a linear top-floor TMDI and demonstrated that for sufficiently flexible isolators, the resulting IR-TMDI configuration is quite effective for suppressing the seismic response of the substructure, while relaxing requirements for TMDI spanning multiple floors.

Building on the above recent developments, this paper extends the work of Liang *et al* [8], which studied the case of linear TMDI for suppressing seismic displacement demands of buildings with linear IS, by considering the IS-TMDI configuration with nonlinear FVD and isolation bearings. These extensions introduce complexity in the optimal TMDI tuning of IS buildings under seismic excitation due to the two distinct sources of nonlinearity. To this end, the paper puts forth a statistical linearization (SL)-based framework for the optimal IS-TMDI tuning to treat the nonlinear devices. The nonlinear FVD is modelled using a power damping force-velocity law commonly traced by commercial FVDs [17], while IS nonlinearity is modelled by the Bouc-Wen hysteretic model [18]. Seismic excitation is modeled as a stationary filtered Kanai-Tajimi stochastic process. The effectiveness of two different optimal IS-TMDI

tuning criteria is comparatively evaluated using a 20-story shear frame building for various IS-TMDI floor placements, including the limiting case of the IR-TMDI.

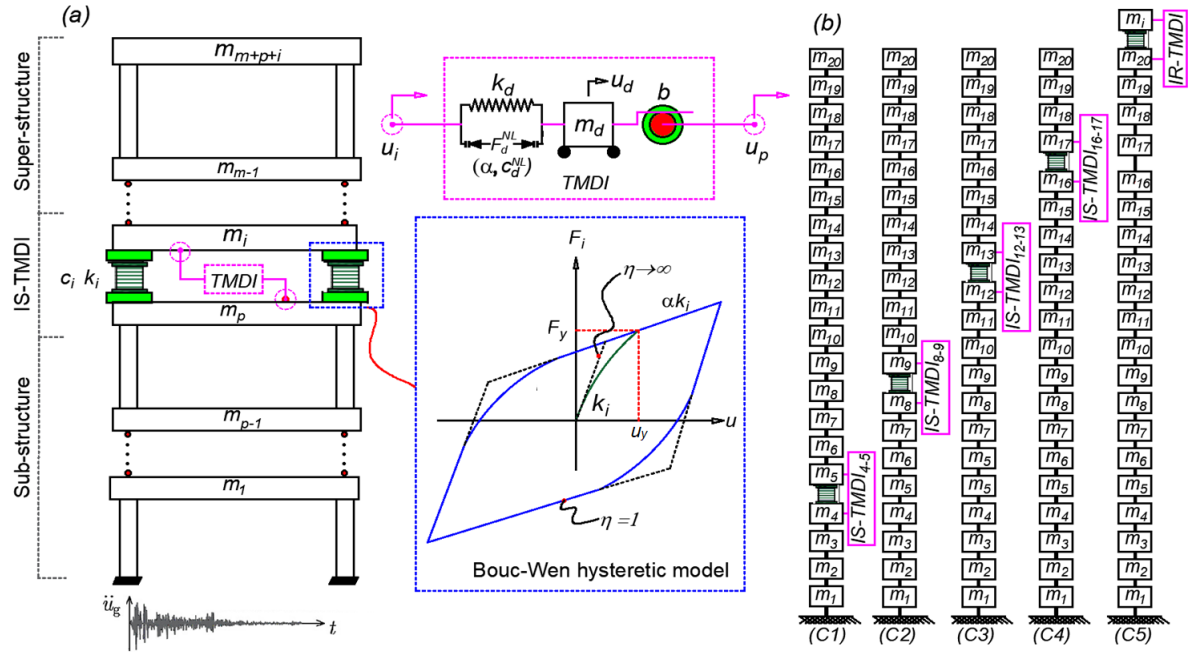

Figure 1: (a) Planar building model equipped with IS-TMDI and (b) different placements of the IS-TMDI used in a benchmark 20-storey.

2 BUILDING MODELING EQUIPPED WITH NONLINEAR IS-TMDI

Consider a generic multi-storey building, modelled as a planar linear damped lumped-mass multi-degree-of-freedom (MDOF) system, subjected to horizontal seismic ground acceleration $\ddot{u}_g$ as shown in Fig. 1(a). The building features an isolated story (IS) at an intermediate i-th floor which divides the structure into two parts: (i) a substructure with p floors lying below the IS and (ii) a superstructure with m floors lying above the IS. In this setting, the considered generic IS-equipped building has m+p+1 stories in total. The IS consists of standard elastomeric bearings (e.g. [19]) exhibiting nonlinear hysteretic behavior under strong ground motion, which is herein captured by the Bouc–Wen model [18], as shown in the inset of Fig. 1(a). Specifically, the resisting force developed across the bearings of the IS is given as

$$F_i = c_i\dot{u} + \alpha_i k_i u + (1-\alpha_i) F_y z \,, \tag{1}$$

where c_i is the IS viscous damping coefficient, k_i is the pre-yielding IS stiffness, α_i is the post-yielding to pre-yielding IS stiffness, F_y is the IS yielding force, and a dot over a symbol denotes time differentiation. Further, in Eq. (1), z is a hysteretic state variable related to the relative displacement (deflection) of the IS, $u = u_i - u_p$, (see Fig.1(a)) through the nonlinear first-order differential equation

$$u_y \dot{z} = A\dot{u} - \gamma|\dot{u}|z|z|^{\eta-1} - \delta\dot{u}|z|^{\eta} \,. \tag{2}$$

In the last equation, u_y is the IS yielding displacement, while δ, γ, η and A are the Bouc-Wen model parameters which control the shape and inclination of the hysteretic force-deformation loops (see also inlet in Fig. 1(a)). In the numerical part of this work, the Bouc-Wen parame-

ters are taken as δ=γ=0.5, η=A=1, and α_i = 0.10, which model a standard smooth hysteretic behaviour, widely adopted in the literature to model elastomeric isolators [20].

Additionally, a TMDI is fitted within the IS, comprising a secondary mass, m_d, connected to the isolated floor via a linear spring with stiffness k_d in parallel with a nonlinear FVD, and to one floor below (p-th floor) via an inerter with inertance b [15]. The latter is modelled as an ideal inerter element developing force $F_b = b\left(\ddot{u}_d - \ddot{u}_p\right)$ [12] where u_d is the displacement of the secondary mass relative to the ground. The FVD is modelled as a nonlinear viscous damper, which is described using the damping power law [17]

$$F_{d,NL} = c_{d,NL}\left|\dot{u}_k\right|^{\alpha} sign\left(\dot{u}_k\right) \tag{3}$$

where $u_k = u_d - u_i$ is the relative displacement across the FVD, *sign(.)* is the signum function, $c_{d,NL}$ is the FVD damping coefficient, and α is a nondimensional damping exponent which varies as $0.05 \leq \alpha \leq 2.0$ in commercial FVD devices (see [15] and references therein).

3 EQUIVALENT LINEAR SYSTEM MODELLING

To facilitate tuning and performance assessment of the nonlinear IS-TMDI presented in Section 2, this study employs statistical linearization (SL) [21,22] to treat the two sources of nonlinear behavior in Eqs. (2) and (3). This treatment supports the definition of an equivalent linear system (ELS) to approximate the response statistics of the nonlinear IS-TMDI equipped building model in Fig.1(a), under ground excitation modelled as a stationary stochastic process. In this manner, estimates of second-order response statistics are found using linear random vibration analysis. The equations of motion of the ELS are written using the x_n (n=1,2,…,p+m+*1*) ELS floor displacements relative to the ground collected in the vector **x**, and the x_k deflection between the secondary mass and the i-th floor displacement as

$$\begin{aligned}
&\mathbf{M}_s\left(\ddot{\mathbf{x}} + \mathbf{r}\ddot{x}_g\right) + \mathbf{C}_s\dot{\mathbf{x}} + \mathbf{K}_s\mathbf{x} + \mathbf{h}z = b\left(\mathbf{R}_i\mathbf{R}_i^T\ddot{\mathbf{x}} + \mathbf{R}_i\ddot{x}_k - \mathbf{R}_p\mathbf{R}_p^T\ddot{\mathbf{x}}\right) + \mathbf{R}_i c_{d,eq}\dot{x}_k + \mathbf{R}_i k_d x_k \\
&m_d\left(\mathbf{R}_i^T\ddot{\mathbf{x}} + \ddot{u}_k + \ddot{u}_g\right) = -b\left(\mathbf{R}_i^T\ddot{\mathbf{x}} + \ddot{x}_k - \mathbf{R}_p^T\ddot{\mathbf{x}}\right) - k_d x_k - c_{d,eq}\dot{x}_k \\
&u_y\dot{z} + C_{eq}\left(\dot{x}_i - \dot{x}_p\right) + K_{eq}z = 0
\end{aligned} \tag{4}$$

In the last equation, $\mathbf{M_s}$, $\mathbf{K_s}$, $\mathbf{C_s}$ are the mass, the stiffness, and the damping matrices of the building, respectively, while **r** is the influence vector of ones, $\mathbf{R}_q$ is a vector of zeros except for the q-th entry which is equal to one and vector **h** is given as

$$\mathbf{h} = \left(1-\alpha_i\right)F_y\mathbf{R}_i - \left(1-\alpha_i\right)F_y\mathbf{R}_p . \tag{5}$$

Further, C_{eq} and K_{eq} are equivalent linear parameters derived by application of SL to the Bouc-Wen model in Eq.(2) as [18]

$$C_{eq} = \sqrt{\frac{2}{\pi}}\left(\gamma\frac{E\left[\dot{x}z\right]}{\sigma_{\dot{x}}} + \delta\sigma_z\right) - A \quad , \quad K_{eq} = \sqrt{\frac{2}{\pi}}\left(\gamma\,\sigma_{\dot{x}} + \delta\frac{E\left[\dot{x}z\right]}{\sigma_z}\right), \tag{6}$$

where $E\left[\dot{x}z\right]$ is the cross variance between the relative velocity of the IS, $\dot{x} = \dot{x}_i - \dot{x}_p$, and the auxiliary state z, and σ_q denotes the standard deviations of the q state. Lastly, $c_{d,eq}$ is the equivalent linear damping coefficient of the nonlinear FVD derived by applying SL to Eq.(3) as

$$c_{d,eq} = 2\xi_{d,eq}\omega_d\left(m_d + b\right) = c_{d,NL}\left(\frac{2^{(5+\alpha)/2}\Gamma\left(2+\alpha/2\right)}{3\sqrt{\pi}\left(1+\alpha\right)}\right)\sigma_{\dot{x}_k}^{\alpha-1} , \tag{7}$$

using an energy-based criterion as detailed in [15], with $\Gamma(.)$ being the gamma function.

In this study, the stochastic ground acceleration $\ddot{u}_g$ is modelled as a white noise process w filtered through a Kanai-Tajimi spectrum representing the soil column properties and a high-pass filter suppressing spurious low-frequency content (e.g. [23]). These filtering operations are expressed in time domain with the aid of displacement coordinates x_f and x_g as

$$\begin{aligned} \ddot{x}_f + 2\xi_f \omega_f \dot{x}_f + \omega_f^2 x_f &= w(t) \\ \ddot{u}_g + 2\xi_g \omega_g \dot{x}_g + \omega_g^2 x_g &= \omega_g^2 x_f \end{aligned} \tag{8}$$

where ω_g and ξ_g are the Kanai-Tajimi parameters associated with the natural frequency and damping ratio of the soil, respectively, and ω_f and ξ_f are the high-pass filter coefficients.

The ELS system in Eq.(4) and the excitation model in Eq.(8) can be readily merged into a single white-noise-driven linear dynamical system with equations of motion cast in state-space [13]. Then, the response covariance matrix of the merged system can be determined by solving an associated Lyapunov system of equations. In the numerical part of the work, this is accomplished by using the `'lyap'` routine of MATLAB®. Notably, the ELS properties in Eqs. (6) and (7) depend on certain second-order response statistics of the merged system (i.e. variances and cross-variances in the response covariance matrix). Therefore, these properties are derived iteratively together with the covariance matrix as per the SL method [21,22].

4 OPTIMAL TUNING OF IS-TMDI

The ELS presented in the previous Section is used for optimal tuning of IS-TMDI, which is further facilitated by defining the dimensionless IS-TMDI properties: TMDI frequency ω_d, equivalent TMDI damping ratio $\xi_{d,eq}$, TMDI mass ratio μ_d, inertance ratio β, IS natural period T_i, and IS critical damping ratio ξ_i, given as

$$\omega_d^2 = \frac{k_d}{b+m_d}\,,\ \xi_{d,eq} = \frac{c_{d,eq}}{2\omega_d(\mu_d+\beta)}\,,\ \mu_d = \frac{m_d}{M_{tot}},\ \beta = \frac{b}{M_{tot}}\,,\ T_i = 2\pi\sqrt{\frac{m_i}{\alpha_i k_i}}\,,\ \text{and}\ \xi_i = \frac{c_i}{2\omega_i m_i}\,, \tag{9}$$

respectively, where M_{tot} is the total mass of the IS-equipped structure. Herein, IS-TMDI tuning is pursued based on the following two different criteria: (i) maximization of the energy dissipated by the TMDI (energy-based tuning) [16], and (ii) minimization of the IS displacement (displacement-based tuning). The underlying objective functions of the above tuning criteria supporting a minimization problem are given as

$$J_1 = 1 - \frac{c_{d,eq}\sigma_{\dot{x}_k}^2}{\left(\sum_{n=1}^{p+m+1} c_n\left(\sigma_{\dot{x}_n}^2 + \sigma_{\dot{x}_{n-1}}^2 - 2E\left[\dot{x}_n\dot{x}_{n-1}\right]\right)\right) + c_{d,eq}\sigma_{\dot{x}_k}^2 + (1-\alpha_i)E\left[\dot{x}z\right]} \quad \text{and} \quad J_2 = \frac{\sigma_{x_i}^2}{\sigma_{x_{unc,top}}^2}, \tag{10}$$

respectively, where $\sigma_{x_{unc,top}}^2$ is the top-floor displacement variance of the uncontrolled building. Then, the IS-TMDI tuning is cast as an optimization problem, seeking to determine optimal TMDI frequency ratio, $\lambda = \omega_d/\omega_s$, where ω_s is the fundamental natural frequency of the IS-equipped structure and optimal equivalent TMDI damping ratio $\xi_{d,eq}$, (primary design variables), given TMDI mass ratio μ_d, inertance ratio β, IS natural period T_i, and IS critical damping ratio ξ_i (secondary design variables), such that J_1 is minimized (energy-based tuning leading to maximization of TMDI energy dissipation) or J_2 is minimized (displacement-based tuning leading to minimization of IS displacement). Mathematically, these can be written as

$$\min_{\mathbf{p}}\left\{J_1(\mathbf{p})\middle|\mathbf{v}\right\} \quad or \quad \min_{\mathbf{p}}\left\{J_2(\mathbf{p})\middle|\mathbf{v}\right\} \quad \text{with} \quad \mathbf{I}_{\text{lb}} \le \mathbf{p} \le \mathbf{I}_{\text{ub}} \tag{11}$$

where $\mathbf{p}=[\lambda\ \xi_{d,eq}]$ is the vector of the primary (free) design variables, with lower and upper bounds $\mathbf{I}_{lb}$ and $\mathbf{I}_{ub}$, respectively, and $\mathbf{v}=[\mu_d\ \ \beta\ T_i\ \xi_i]$ is the vector of the secondary (fixed) design variables.

The optimization problems in Eq.(11) are numerically solved using the pattern search algorithm as implemented in the built-in MATLAB® command `'patternsearch'` with sufficiently wide search ranges $\mathbf{I}_{lb}$ = [0 0] and $\mathbf{I}_{ub}$ = [2 4], such that the design variables do not hit the boundaries of the search domain.

5 NUMERICAL APPLICATIONS

For numerical illustration of the IS-TMDI tuning and performance assessment, a 20-storey shear frame building is used with a common floor mass of 300t, a floor stiffness of 1.0e9N/m, and a floor damping coefficient of 2.261e6 Ns/m. This structure has been previously considered as a benchmark to assess the effectiveness of the TMD [24] and of the TMDI [25] for seismic response mitigation of base-isolated buildings. Herein, the considered structure is modified to define four different IS-TMDI placement cases as shown in Figure 1(b): case 1 (C1) between floor masses m_4 and m_5; case 2 (C2) between floor masses m_8 and m_9; case 3 (C3) between floor masses m_{12} and m_{13}; and case 4 (C4) between floor masses m_{16} and m_{17}. An additional case 5 (C5) is further examined that considers the IR-TMDI of Rajana and Giaralis [16] whereby an extra service/fake isolated floor with mass m_i= 300t (i.e., equal to the mass of a typical floor) is added on top of the benchmark structure in which a TMDI is installed. In all cases, a very small TMDI mass ratio is used, μ_d = 0.1%, representing the self-weight of the TMDI devices and connections, while the IS damping ratio is taken as ξ_i =5%, and a relatively long isolation period, T_i =4s, is adopted for which the IR-TMDI performed well as reported in [16] for the case of primary structures modelled as single-degree-of-freedom systems. Further, the excitation is represented by the filtered Kanai-Tajimi spectrum with properties ω_g = 5.34 rad/s, ζ_g = 0.88, ω_f = 2.12 rad/s, and ζ_f = 1.17 in Eq.(8), representing soft soil conditions as per [26], with peak ground acceleration set at 0.3g.

Figure 2 reports the optimal ratio $c_{d,NL}/c_{d,eq}$ (nonlinear damping coefficient of the FVD over the linearized FVD damping coefficient) obtained from Eq.(7) for damping exponents α ranging from 0 to 2, by solving the optimal IS/IR-TMDI tuning problems in Eq.(10) for two different inertance ratios β = 2% and 10%. Note that the value of α=1 corresponds to the linear FVD for which $c_{d,NL}$= c_d= $c_{d,eq}$ in all the cases. Therefore, the plots in Fig.2 quantify the difference of the FVD damping coefficient from the optimal equivalent damping, $c_{d,eq}$, found by solving the optimal tuning problem using the ELS as the FVD deviates from linearity. It is found that this difference (i.e., the ratio $c_{d,NL}/c_{d,eq}$) is generally higher for the low inertance ratio value, while it monotonically increases with α for the C1 and C2 cases (lowest IS-TMDI floor placements), and monotonically reduces with α for the C4 and C5 cases (highest IS-TMDI placement and top-floor placement). Further, the general trends of the $c_{d,NL}/c_{d,eq}$ with α curves are not affected much by the tuning criterion (objective function) in Eq. (10). Whilst the data in Fig.2 do not necessarily correlate with the seismic response mitigation performance of the IS/IR-TMDI (see [15]), they do demonstrate that the $c_{d,NL}/c_{d,eq}$ ratio takes on significantly different values from unity as α deviates from 1 which highlights the usefulness of the proposed SL-based framework for IS-TMDI tuning accounting for FVD nonlinearity.

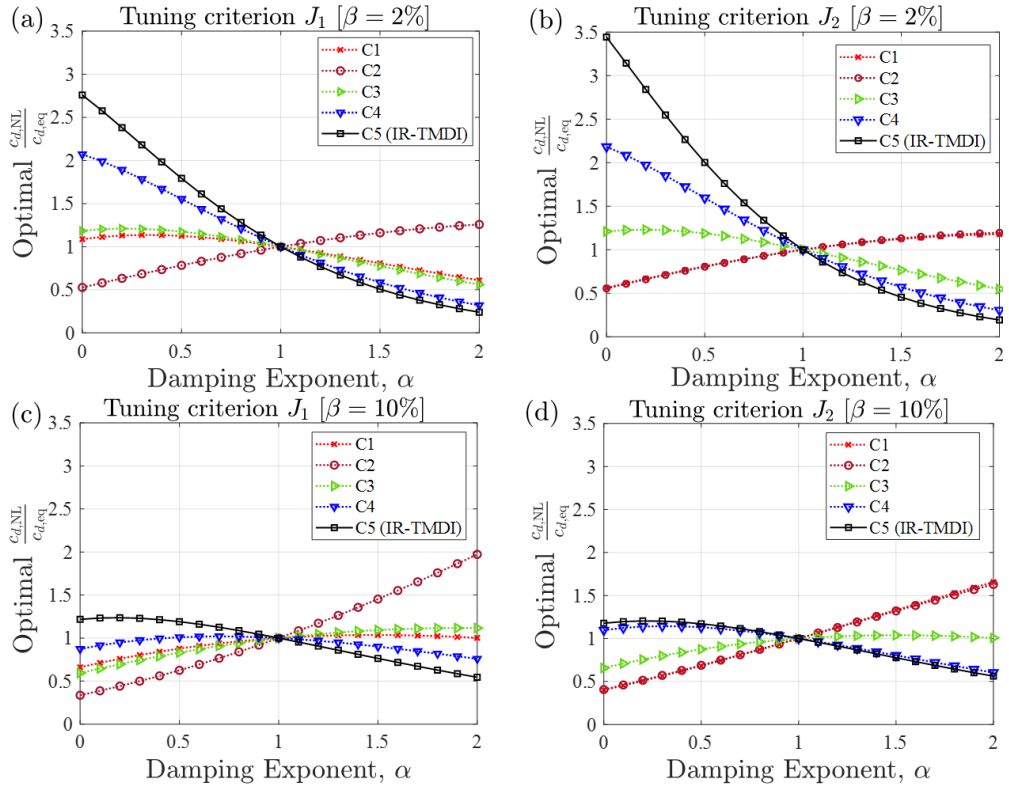

Figure 2: Optimal damping coefficient ratios as functions of the nonlinear FVD exponent in Eq.(2) for the two tuning criteria in Eq.(10) and two different inertance ratio values.

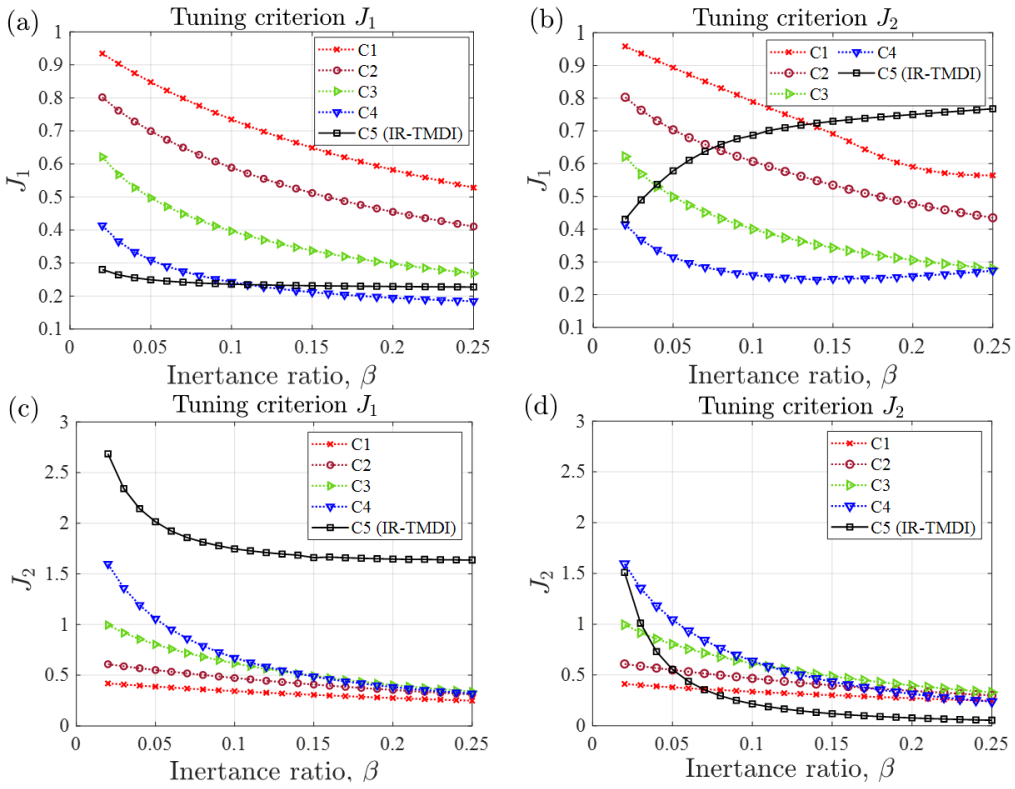

Figure 3: Optimal objective function values in Eq.(10) for varying inertance ratio for energy-based (J_1) and displacement-based (J_2) IS/IR-TMDI optimal tuning.

To gain insights on the comparative significance of the two different tuning criteria in Eq.(10) used for optimal IS/IR-TMDI design, Fig. 3 reports the achieved values of J_1 and J_2 derived by solving the optimization problem in Eq.(11) as a function of the inertance ratio β. Consistent J_1 and J_2 performances are found for the four IS-TMDI cases: improved performance is noted (i.e. increased TMDI energy dissipation and reduced IS displacement, J_2) as the IS-TMDI is placed in lower floors and/or as the inertance ratio increases, with the exception of IS displacement of the J_2-optimized C4 case (highest IS-TMDI floor placement case), which slightly increases for β>15% in Fig.3(b). Still, these improvements saturate with the inertance ratio. Moreover, the achieved J_1 and J_2 performances are not significantly influenced by the adopted tuning criterion, with the same exception case discussed above.

On the antipode, J_1 and J_2 performances for the IR-TMDI case (i.e. top-floor IS-TMDI) are heavily influenced by the adopted tuning criterion, as previously reported by the authors for the case of SDOF primary structures [16]. In fact, for the displacement-based J_2 tuning, TMDI energy dissipation reduces with inertance (i.e. J_1 increases/deteriorates) in Fig.3(b). This generally opposing trend for J_1 and J_2 for the IR-TMDI can be attributed to a reduced TMDI engagement as IS displacement reduces, leading to reduced TMDI energy dissipation, which is not the case for the IS-TMDI configurations (with the exception of the C4 case where IS-TMDI is closer to the building top). Similarly, Fig.3(c) shows that an energy-based tuning of the IR-TMDI poses significantly higher IS displacement demands compared to all the IS cases. In this context, IS-TMDI placement to lower floors appears to be beneficial for a robust performance against tuning criteria. Still, the IR-TMDI (C5 case) performs best in terms of TMDI energy dissipation against all IS-TMDI cases for energy-based tuning (with the exception of the C4 IS-TMDI case for β>14%) in Fig.3(a) and in terms of IS displacement for displacement-based tuning for β>7% in Fig.3(d). In this regard, the performance assessment of IS/IR-TMDI configurations and tuning criteria calls for examining the response of the building, as considered in Figs. 4 and 5 using displacement response statistics from stochastically excited ELSs with optimized IS/IR-TMDI.

Figure 4 plots the floor displacement variance at each floor of the 20-storey benchmark building equipped with IS/IR-TMDI optimally tuned using the two different tuning criteria in Eq.(10) and for two different inertance ratios β = 2% and β = 10%. To facilitate a meaningful comparison, the floor displacement variances are normalized by the top-floor displacement variance of the benchmark uncontrolled structure (no IS-TMDI), while displacement variances for the uncontrolled structure are also included. Data for the four IS-TMDI configurations confirm that the tuning criterion has insignificant influence to the displacement control capacity of the IS-TMDI. Nevertheless, the inertance ratio is an important design consideration and needs to be sufficiently high to suppress IS displacement. It is found that for β=10% floor displacement of the IS-TMDI equipped structure is always lower from the uncontrolled structure, while this is not the case for C3 and C4 configurations for the relatively low β=2% inertance value examined. Further, it is confirmed that lower floor IS-TMDI placement is more advantageous in controlling floor displacements. More importantly, irrespective of placements and inertance value, all the IS-TMDI configurations are quite effective in suppressing floor displacements at all floors other than the special isolated floor. At the same time, expectedly, the tuning criterion for the IR-TMDI case does influence significantly the overall structural performance. It is clearly seen that the energy-based tuning leads to much improved displacement control performance throughout the building height. More importantly, the IS-TMDI outperforms the IR-TMDI in suppressing floor displacement at all the substructure levels (i.e. below the isolated floor), indicating a potential superiority of IS-TMDI as long as the IS displacement is within acceptable ranges, regulated by the inertance ratio.

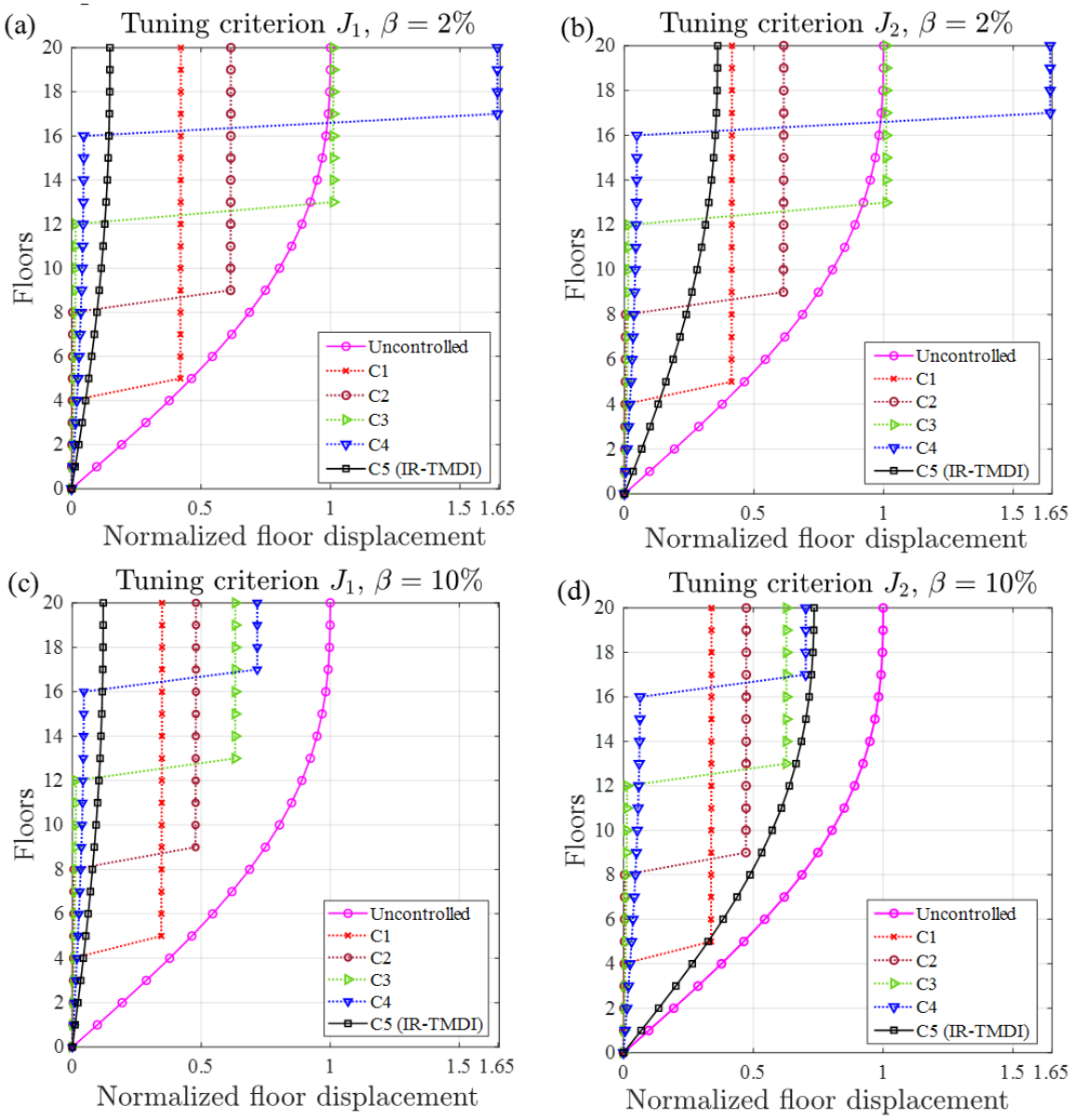

Figure 4: Floor displacement variance normalized to the top-floor displacement of the uncontrolled structure achieved for energy-based (J_1) and displacement-based (J_2) IS/IR-TMDI optimal tuning.and for two different inertance ratio values β = 2% and β = 10%.

To examine the seismic structural damage mitigation potential of the IS/IR-TMDI, Fig.(5) plots inter-storey drifts for the same cases as in Fig.4, normalized by the inter-storey drift of the uncontrolled structure at each corresponding floor. The drift of the special isolated floor is not plotted as the focus is now on the seismic drift demands posed to the building. discontinuity is shown in the plots at the isolation layer position to enhance visualization of the building's drift demands. Results suggest that the increase of the inertance ratio does not improve structural drift performance, contrary to the case of IS displacement. Moreover, it is found that IS-TMDI consistently outperforms the IR-TMDI throughout the building height irrespective of tuning criterion and inertance ratio. Lastly, it is seen that IS-TMDI placement at the lower floors achieves more effective storey-drift reductions for the entire building height.

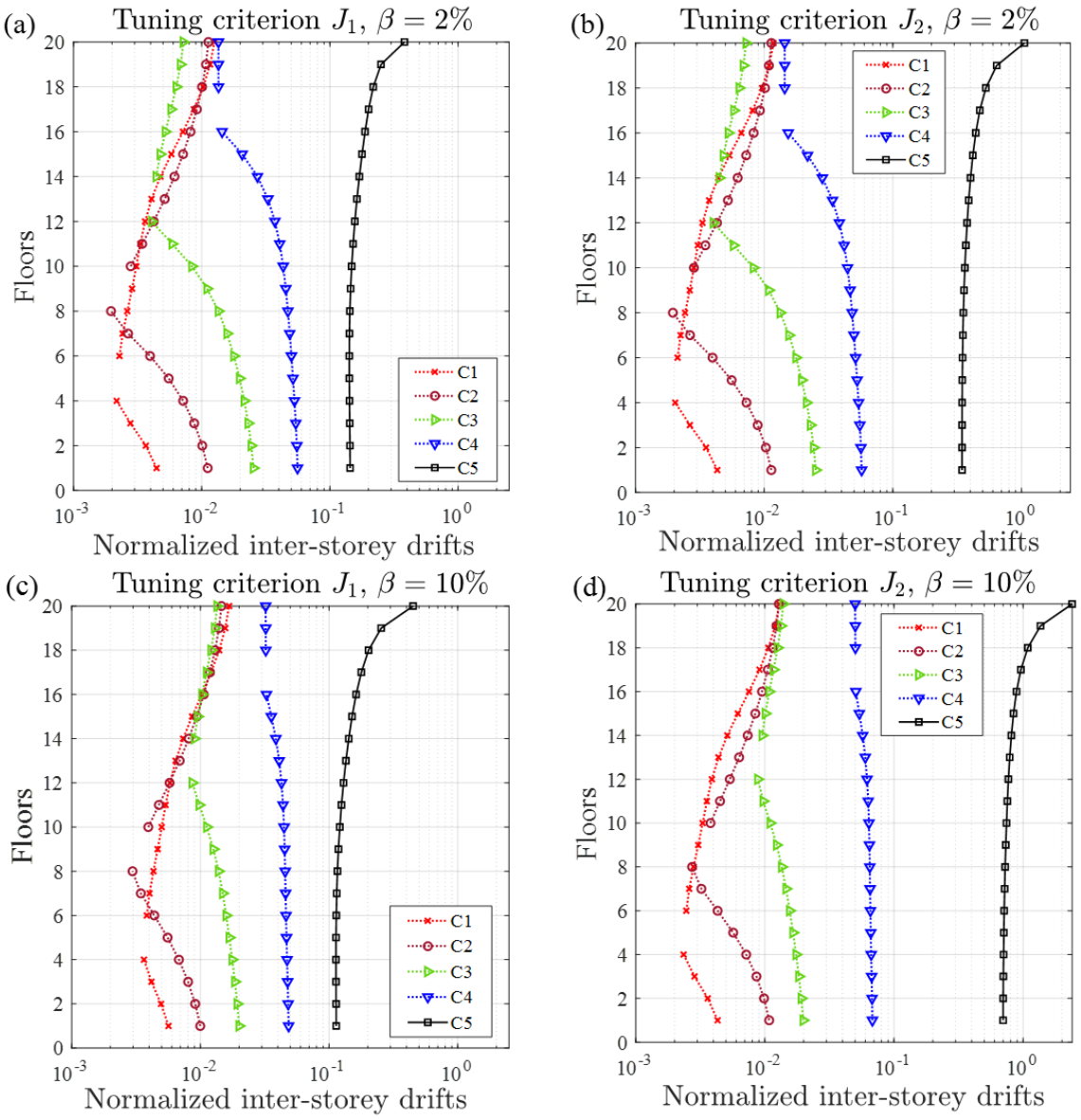

Figure 5: Inter-storey drifts variance at each floor level for both performance functions and different inertance ratios (e.g., β =2% and 10%)

6 CONCLUDING REMARKS

This paper offered a pilot investigation of the potential of IS-TMDI with nonlinear isolators and viscous damper for the seismic protection of multi-storey buildings. This has been pursued by adopting a 20-storey building previously used in the literature for benchmarking the potential of the TMD(I) to mitigate displacement demands in base isolated buildings. Four different IS-TMDI placements have been considered together with a limiting top-floor IR-TMDI configuration, previously studied by authors for the case of SDOF buildings. Statistical linearization was adopted to treat the nonlinear forces of the IS/IR-TMDI isolators and viscous damper by establishing analytically equivalent linear systems (ELSs), approximating response variances of the nonlinear systems under stationary Kanai-Tajimi excitation. These response estimates were used for optimal IS/IR-TMDI tuning based on two different criteria,: maximization of TMDI energy dissipation and minimization of IS displacement, as well as for performance assessment of optimal IS/IR-TMDI equipped benchmark structure. Numerical

results demonstrate that the ELS-based tuning approach is effective for determining TMDI stiffness and nonlinear damping properties. They also show that IS-TMDI tuning and performance is insensitive to the choice of tuning criteria, contrary to IR-TMDI. Further, reported floor displacement and storey-drift data suggest that the low-floor IS-TMDI placements are more efficient in seismic response mitigation of the considered building, while sufficient inertance needs to be provided to regulate the IS displacement demands. Further promising computational and experimental research is warranted to shed further light on the IS-TMDI capability for mitigating seismic demands under recorded ground motions.

REFERENCES

[1] Naeim, F. and Kelly, J.M. Design of seismic isolated structures: from theory to practice. John Wiley & Sons, (1999).

[2] Faiella, D.and Mele, E. Insights into inter-story isolation design through the analysis of two case studies. *Engineering Structures* (2020) **215**: 110660.

[3] Faiella, D. and Mele, E. Vibration characteristics and higher mode coupling in intermediate isolation systems (IIS): a parametric analysis. *Bulletin of Earthquake Engineering* (2019) **17**: 4347–4387.

[4] Villaverde, R. Aseismic roof isolation system: feasibility study with 13-story building. *Journal of Structural Engineering* (2002) **128**(2): 188–196.

[5] Matta, E. and De Stefano, A. Seismic performance of Pendulum and translational roof-garden TMDs. *Mechanical Systems and Signal Processing* (2009) **23**(3): 908–921.

[6] Liu, Y., Wu, J. and Donà, M. Effectiveness of fluid-viscous dampers for improved seismic performance of inter-storey isolated buildings. *Engineering Structures (*2018) **169**: 276–292.

[7] Politopoulos, I. A review of adverse effects of damping in seismic isolation. *Earthquake Engineering and Structural Dynamics* (2008) **37**(3): 447–465.

[8] Liang, Q., Wei, J. and Li, L. Seismic Control of Story Isolation System Using Tuned Mass Damper Inerter. *Journal of Engineering Mechanics* (2023) **149**(3):04023012.

[9] Marian, L. and Giaralis, A. Optimal design of a novel tuned mass-damper-inerter (TMDI) passive vibration control configuration for stochastically excited structures. *Probabilistic Engineering Mechanics* (2014) **38**: 156–164.

[10] Smith, M.C. Synthesis of mechanical networks: The inerter. *IEEE Transactions on Automated Control* (2002) **47**(10): 1648–1662.

[11] Nakaminami, S., Kida, H., Ikago, K. and Inoue, N. Dynamic testing of a full-scale hydraulic inerter-damper for the seismic protection of civil structures. *7th International Conference on Advances in Experimental Structural Engineering* (2017) Pavia: 41–54.

[12] Smith, M.C. The inerter: a retrospective. *Annual Review of Control, Robotics, and Autonomous Systems* (2020) **3**: 361–391.

[13] Giaralis, A. and Taflanidis, A.A. Optimal tuned mass-damper-inerter (TMDI) design for seismically excited MDOF structures with model uncertainties based on reliability criteria. *Structural Control and Health Monitoring* (2018) **25**(2): e2082.

[14] Taflanidis, A.A., Giaralis, A. and Patsialis, D. Multi-objective optimal design of inerter-based vibration absorbers for earthquake protection of multi-storey building structures. *Journal of the Franklin Institute* (2019) **356**(14): 7754–7784.

[15] Rajana, K., Wang, Z. and Giaralis, A. Optimal design and assessment of Tuned Mass Damper Inerter with nonlinear viscous damper in seismically excited multi-storey buildings. *Bulletin of Earthquake Engineering* (2023) **21**: 1509–1539.

[16] Rajana, K. and Giaralis, A. A novel nonlinear isolated rooftop tuned Mass Damper-inerter (IR-TMDI) system for seismic response mitigation of buildings. *Acta Mechanica* (2023) **234**(9): 3751–3777.
[17] Seleemah, A. A. and Constantinou, M. C. Investigation of seismic response of buildings with linear and nonlinear fluid viscous dampers. *Technical Report NCEER-97-0004.* (1997) Buffalo, NY: National Earthquake Engineering Research Center.
[18] Wen, Y.K. Equivalent linearization for hysteretic systems under random excitation. *Journal of Applied Mechanics* (1980) **47**(1): 150–154.
[19] Ryan, K.L. and Earl, C.L. Analysis and design of inter-story isolation systems with non-linear devices. *Journal of Earthquake Engineering* (2010) **14**(7): 1044–1062.
[20] De Domenico, D. and Ricciardi, G. Optimal design and seismic performance of tuned mass damper inerter (TMDI) for structures with nonlinear base isolation systems. *Earthquake Engineering and Structural Dynamics* (2018) **47**(12): 2539–2560.
[21] Roberts, J. and Spanos, P. Random vibration and statistical linearization. John Wiley & Sons Ltd, (1991).
[22] Mitseas, I.P., Kougioumtzoglou, I.A., Giaralis, A. and Beer, M. A novel stochastic linearization framework for seismic demand estimation of hysteretic MDOF systems subject to linear response spectra. *Structural Safety* (2018) **72**: 84-98.
[23] Spanos, P.D., Giaralis, A. and Jie L. Synthesis of accelerograms compatible with the Chinese GB 50011-2001 design spectrum via harmonic wavelets: artificial and historic records. *Earthquake Engineering and Engineering Vibrations* (2009) **8**: 189-206.
[24] Yang, J.N., Danielians, A. and Liu, S.C. Aseismic hybrid control systems for building structures. *Journal of Engineering Mechanics* (1991) **117**(4): 836–853.
[25] Masnata, C., Di Matteo, A., Adam, C. and Pirrotta, A. Assessment of the tuned mass damper inerter for seismic response control of base-isolated structures. *Structural Control and Health Monitoring* (2021) **28**(6):e2736.
[26] Giaralis, A. and Spanos, P.D. Derivation of response spectrum compatible non-stationary stochastic processes relying on Monte Carlo peak factor estimation. *Earthquakes and Structures* (2012) **3**: 581-609.